Supporting Information

Marklewitz et al. 10.1073/pnas.1502036112

SI Methods

Mosquito Collection and Species Identification. Mosquitoes were trapped in forest edge habitats in Taï National Park, Côte d'Ivoire, as previously described (1). Mosquito species were identified by morphologic criteria (2–4). Female mosquitoes (n = 4,839) were divided into 432 pools (1–50 specimen per pool) according to mosquito species, sex, and sampling location (1).

Virus Isolation, Purification, and Growth. Virus isolation was performed in C6/36 (*Aedes albopictus*) cells (5) and in Vero E6 (*Ceropithecus aethiops*) cells, as described before (6). Briefly, mosquito pools were homogenized and 100 μL of the clarified supernatant was used to infect the cells. The viruses in this study were three times endpoint-diluted, and virus stocks of the eighth passage of FERV (isolate C51/CI/2004) and the ninth passage of JONV (isolate B81/CI/2004) were used for further analyses. Virus titers were determined by tissue culture infectious dose 50 in C6/36 cells (7). For virus growth kinetics, C6/36 cells were infected in doublets at MOI of 0.1 and 0.01 (8). Aliquots of infectious cell culture supernatant were harvested every 24 h for periods of 5 d, and viral genome copies were quantified by real-time RT-PCR [FERV-F 5′-TCAGCTAGTCAGATACCATCAATAC, FERV-R 5′-CAATGTTACTACAGTCGGCTTTTTTG, FERV-TM 5′-6-carboxyfluorescein(FAM)-CCCAATATGCAAGATTCAGGGACAGAA-BHQ1; JONV-F 5′-TGCTTCGGAAGGAGCTCTCTA, JONV-R 5′-TGTATGGCTCAAGTGCCTCTAATC, JONV-TM 5′-6-FAM-AGGAAAAAGCAAGTCAGCACTCCTCGCBHQ1]. The detection limit of each assay is below 10,667 viral genome copies per milliliter (projected).

Cell Culture Infection Experiments. African green monkey kidney epithelial cells (Vero E6), baby hamster kidney fibroblasts (BHK-21), human hepatocellular carcinoma cells (HuH-7), horseshoe bat lung cells (RhiLu/1) (9), Aba roundleaf bat lung cells (HipaLu/24), kidney cells from goats (*Capra hircus*) (ZN-R), lung cells from Lesser white-toothed shrew (Crocsu-Lu) (10), and cells derived from grass frog embryos (*Rana pipiens*) (ICR-2a) were infected with JONV or FERV at an MOI of 10. Cell culture supernatants were passaged in fresh cells every 7 d in a 1–10 dilution for three consecutive passages. Supernatants from passages 0, 1, and 3 were tested for virus replication by real-time RT-PCR.

To assess temperature sensitivity, C6/36 cells were infected with JONV, FERV, GOLV, HEBV, LACV, or RVFV at an MOI of 0.1 and cultured under temperature gradients from 29 to 34 °C for 3 d, respectively. Vero E6 cells were infected with JONV, FERV, LACV, or RVFV at an MOI of 10 and incubated at 30 °C. Mock infected cells were incubated at 29, 33, and 34 °C. RNA was extracted from cell culture supernatants 0, 24, 48, and 96 hpi. Viral genome copies and actin gene copies were quantified by real-time RT-PCR.

Electron Microscopy. Virions were sedimented through a 36% (vol/vol) sucrose cushion by ultracentrifugation, resuspended in PBS, and fixed with 2% (vol/vol) paraformaldehyde (11, 12). For ultrathin sections, infected cells were fixed with 2.5% (vol/vol) glutaraldehyde, enclosed in low-melting agar, and embedded in resin (11, 12). Virions were analyzed by transmission electron microscopy.

Genome Sequencing. Full-genome sequencing of JONV (isolate B81/CI/2004) and FERV (isolate C51/CI/2004) was done by a combination of deep sequencing via 454-pyrosequencing on a GS Junior Platform (Roche) (8) and random-primed RT-PCR optimized for the detection of encapsidated nucleic acids (6, 13). Briefly, after RNA extraction, double-stranded cDNA was synthesized with random hexamers linked to an anchor sequence (5′-GACCATCTAGCGACCTCCAC). Amplification was performed with anchor-specific oligonucleotides by PCR. The PCR product was cloned into the pCR2.1 TOPO vector (Life Technologies). Clones were analyzed by PCR and Sanger-sequenced. Sequences were assembled using Geneious v6 (14). Fragment-specific oligonucleotides were used to close sequence gaps by PCR. The 3′ and 5′ genome termini were confirmed by RACE-PCR using the 5′ RACE Kit (Life Technologies). Additional full-genome sequences of JONV and FERV isolates were generated by deep sequencing on an Ion Torrent PGM platform (Life Technologies) according to the manufacturer's instructions. Reads were identified by reference mapping to JONV B81/CI/2004 and FERV C51/CI/2004, respectively, and whole genomes were generated under visual inspection in Geneious (14).

Virus Prevalence Screening and Sequence Generation. C6/36 cell cultures were screened for the presence of JONV and FERV with virus-specific real-time RT-PCR (1). From all JONV- or FERV-positive mosquito pools, a genome fragment comprising the palm domain of the RNA-dependent RNA polymerase (RdRp) was amplified by nested PCR. Primers for the first PCR were JONV-F1 5′-TGGATCATGGACACAAGGCCACTC and JONV-R1 5′-GCCCTCTTGGCAGTAAGCCACC, and FERV-F1 5′-AACCACAGCAATGCTATCTGGGC and FERV-R1 5′-AACCACAGCAATGCTATCTGGGC, respectively. Nested PCR was performed with JONV-F2 5′-GGAAGGGCTGCATATCAAGGG and JONV-R2 5′-CCCTGCATCCAACCAATCCTACC, or FERV-F2 5′-CAGGTCATCAAGGAATACCCAGAG or FERV-R2 5′-CCAACCTGCTACTCCTCTTATGCT, respectively. The PCR products were Sanger-sequenced after purification.

Genome and Phylogenetic Analyses. The genome was analyzed by comparison of the nucleotide and amino acid sequences with other sequences of the GenBank database (www.ncbi.nlm.Nih.gov/Genbank), using BLASTn and BLASTx. Conserved protein motifs were identified by web-based comparison with the Pfam database (pfam.xfam.org/). Putative signal peptide cleavage sites were identified with the SignalP prediction server (www.cbs.dtu.dk/services/SignalP). Hydrophobic and potential transmembrane-spanning regions were predicted by transmembrane helices in proteins (TMHMM) (www.cbs.dtu.dk/services/TMHMM-2.0), and *N*-linked glycosylation sites were identified using the NetNGlyc 1.0 server (www.cbs.dtu.dk/services/NetNGlyc).

For phylogenetic analysis, complete RdRp protein sequences were aligned with representative sequences of other bunyaviruses, using the Expresso structural alignment algorithm on the TCoffee webserver (tcoffee.crg.cat) (15). The alignment was manually inspected, and poorly aligned columns were removed, resulting in a final alignment of 411 amino acids. For phylogenetic analyses including outgroups, complete translated ORFs of arenavirus L segments and concatenated translated ORFs of othomyxovirus segments encoding the PA and pb1 proteins were added to the stripped bunyavirus alignment and aligned using multiple sequence alignment based on fast Fourier transform (MAFFT) and the E-INS-I algorithm (16). The alignment was reduced to conserved columns consisting of 270 amino acids (Fig. S4). Phylogenetic analyses were performed using PhyML and the Blosum62 substitution model in Geneious v6 (14), with confidence testing based on 1,000 bootstrap iterations.

Phylogenetic analyses of JONV and FERV isolates were based on a 1,020-nt sequence alignment comprising the conserved RdRp motifs. Maximum likelihood analyses were performed using the GTR model with 1,000 replicates in Geneious v6 (14).

Ancestral State Reconstruction. Parsimony-based ancestral state reconstruction was done in Mesquite, using the ancestral state reconstruction package (17) and the informed trait characteristics shown in Table S1. Maximum likelihood-based ancestral state reconstruction and hypotheses testing was done in Bayestraits (18). The trait change matrix was based on four states that were composed of two uncorrelated binary traits occurring in combination (state 1 = no insect host, no vertebrate host; state 2 = no insect host, vertebrate host; state 3 = insect host, no vertebrate host; state 4 = dual hosts) (Table S1). Transition likelihoods between all four states were left independent. For hypotheses testing, ancestral host assumptions were fixed at tree nodes of interest, and maximum likelihood values for trait change matrices achieved after 1,000 optimization attempts were recorded across 1,000 bootstrap replicates of ML trees. The relative likelihoods between models using a fixed host assumption and the null model (no fixed assumptions) were expressed as "loss of likelihood" against the null model (there was always a loss). This approach corresponds to a likelihood ratio test, which for the case of nested models is likelihood ratio = 2[log-likelihood (better fitting model) − log-likelihood (worse fitting model)]. With likelihood ratio > 2 conventionally being considered significant, a relative likelihood of 1 log (corresponding to a 10-fold loss of likelihood) was considered as the threshold of significance. All analyses were replicated on 1,000 bootstrap versions of the ML trees shown in Fig. S8 *A*–*C*.

mRNA Analyses. C6/36 cells were infected with JONV and FERV at an MOI of 0.1 and harvested 24 hpi. mRNA was extracted using the RNeasy total RNA Extraction Kit (Qiagen) and analyzed by Northern blotting, as described previously (8, 19). Specific DIG-labeled PCR probes were generated using the primers JONV-L-F 5′-GGAAGGGCTGCATATCAAGGG, JONV-L-R 5′-CATTTTGCCTACATTGTCAGACTCAG, JONV-M-F 5′-GAGGAAGATGTAGTCAGCGAGGGAGG, JONV-M-R 5′-ACTTCAACTCCAGCAACGTGTTCG, JONV-S1-F 5′-TGCGTACAGTTGCCTTCCGG, JONF-S1-R 5′-ACCTCGCAAGTATCAGCTTACGC, JONV-S2-F 5′-CTGTTTTGGCTATGTTACCGCAGGC, JONV-S2-R 5′-GTCTATTTGGCGTTGGATTTCAGCAAG, FERV-L-F 5′-TGCTAGAAGAGGCAGATATGTTGTGGG, FERV-L-R 5′-TCCCTGGTTCACCTTCAATACGG, FERV-M-F 5′-AGTAAACCTTGATTTCACCATGTCTGCTC, FERV-M-R 5′-GCAGTTTGTCAATGTTGTTAAAGCTTG, FERV-S1-F 5′-CGCATTACGTGTGATTCGTACTCG, FERV-S1-R 5′-AATTGTCAGACCTTGGTAATTAGCCTCC, FERV-S2-F 5′-CAGCTTCAGGCAGATCACTGTGC, and FERV-S2-R 5′-AGTGCCTTGATGTTGCTGTCTGTC.

To discriminate between vRNA and mRNA, JONV-infected cells were harvested 0, 3, 6, 15, and 24 hpi, and RNA was extracted. Hot-started strain-specific cDNA was synthesized using either a forward primer (5′-GAACACGTTGCTGGAGTTG) or a reverse primer (5′-TACCCACAGTCCTTGCTTGTTC). Amounts of positive- and negative-sense viral RNA were quantified by real-time PCR using the primers JONV-F-M 5′-TGGGTGAAGCTAGGGTAGAAGTAGA and JONV-R-M 5′-GTCAGACCATCCAGTGTAAAAACCT and the probe JONV-TM-M 5′-6-FAM-AGCCACTTGGCAACTCATACACGGTTCA-BHQ2.

Protein Analyses. Viral proteins were analyzed as previously described (20). Briefly, viral particles were purified by saccharose gradient ultracentrifugation. Viral proteins were either lysed directly or deglycosylated using peptide-*N*-glycosidase F (New England BioLabs) and subsequently lysed in 4xNuPage LDS Sample Buffer (Life Technologies) at 70 °C for 10 min. Proteins were separated by SDS/PAGE on a NuPAGE Novex 4–12% (vol/vol) Bis Tris gel with NuPAGE MES SDS Running Buffer (Life Technologies) and visualized by Coomassie blue (R-250) staining. Proteins were analyzed by limited tryptic digestion and mass spectrometry using MALDI-TOF and liquid chromatography mass spectrometry (LC-MS). N-terminal amino acid sequencing was performed by Edman degradation, as previously described (20).

Nucleotide Sequence Accession Numbers. Complete genome sequences of JONV and FERV viruses were assigned GenBank accession numbers KP710232, KP710238-KP710245 and KP710246, KP710262-KP710269, respectively. Further sequence fragments from JONV and FERV strains were assigned to GenBank accession numbers KP710233–KP710237 and KP710247–KP710261, respectively.

1. Junglen S, et al. (2009) Examining landscape factors influencing relative distribution of mosquito genera and frequency of virus infection. *EcoHealth* 6(2):239–249.
2. Edwards FW (1941) *Mosquitoes of the Ethiopian Region - III. Culicine adults and pupae* (Oxford University Press, London).
3. Jupp PG (1996) Mosquitoes of South Africa: Culicinae and Toxorhynchitinae (Ekogilde Publishers, Hartebeespoort, Repubulic of South Africa).
4. Gillies MT, De Meillon B (1968) *The Anophelinae of Africa south of the Sahara (Ethiopian Zoogeographical Region)* (South Africa Institute for Medical Research, Johannesburg), 2nd Ed, pp 343.
5. Igarashi A (1978) Isolation of a Singh's Aedes albopictus cell clone sensitive to Dengue and Chikungunya viruses. *J Gen Virol* 40(3):531–544.
6. Junglen S, et al. (2009) A new flavivirus and a new vector: Characterization of a novel flavivirus isolated from uranotaenia mosquitoes from a tropical rain forest. *J Virol* 83(9):4462–4468.
7. Reed LJ, Muench H (1938) A simple method of estimating fifty percent endpoints. *Am J Hyg* 27:493–497.
8. Zirkel F, et al. (2011) An insect nidovirus emerging from a primary tropical rainforest. *MBio* 2(3):e00077–11.
9. Hoffmann M, et al. (2013) Differential sensitivity of bat cells to infection by enveloped RNA viruses: Coronaviruses, paramyxoviruses, filoviruses, and influenza viruses. *PLoS ONE* 8(8):e72942.
10. Eckerle I, et al. (2014) Replicative Capacity of MERS Coronavirus in Livestock Cell Lines. *Emerg Infect Dis* 20(2):276–279.
11. Biel SS, Gelderblom HR (1999) *Electron microscopy of viruses* (Oxford University, Oxford, United Kingdom).
12. Hayat MA (2000) *Principles and techniques of electron microscopy: Biological applications* (Macmillan Press Houndmills, London).
13. Stang A, Korn K, Wildner O, Uberla K (2005) Characterization of virus isolates by particle-associated nucleic acid PCR. *J Clin Microbiol* 43(2):716–720.
14. Kearse M, et al. (2012) Geneious Basic: An integrated and extendable desktop software platform for the organization and analysis of sequence data. *Bioinformatics* 28(12):1647–1649.
15. Notredame C, Higgins DG, Heringa J (2000) T-Coffee: A novel method for fast and accurate multiple sequence alignment. *J Mol Biol* 302(1):205–217.
16. Katoh K, Standley DM (2013) MAFFT multiple sequence alignment software version 7: Improvements in performance and usability. *Mol Biol Evol* 30(4):772–780.
17. Maddison WP, Maddison DR (2014) Mesquite: A modular system for evolutionary analysis. Available at mesquiteproject.org. Accessed April 14, 2015.
18. Pagel M, Meade A, Barker D (2004) Bayesian estimation of ancestral character states on phylogenies. *Syst Biol* 53(5):673–684.
19. Marklewitz M, et al. (2013) Discovery of a unique novel clade of mosquito-associated bunyaviruses. *J Virol* 87(23):12850–12865.
20. Zirkel F, et al. (2013) Identification and characterization of genetically divergent members of the newly established family Mesoniviridae. *J Virol* 87(11):6346–6358.
21. Delport W, Poon AF, Frost SD, Kosakovsky Pond SL (2010) Datamonkey 2010: A suite of phylogenetic analysis tools for evolutionary biology. *Bioinformatics* 26(19):2455–2457.

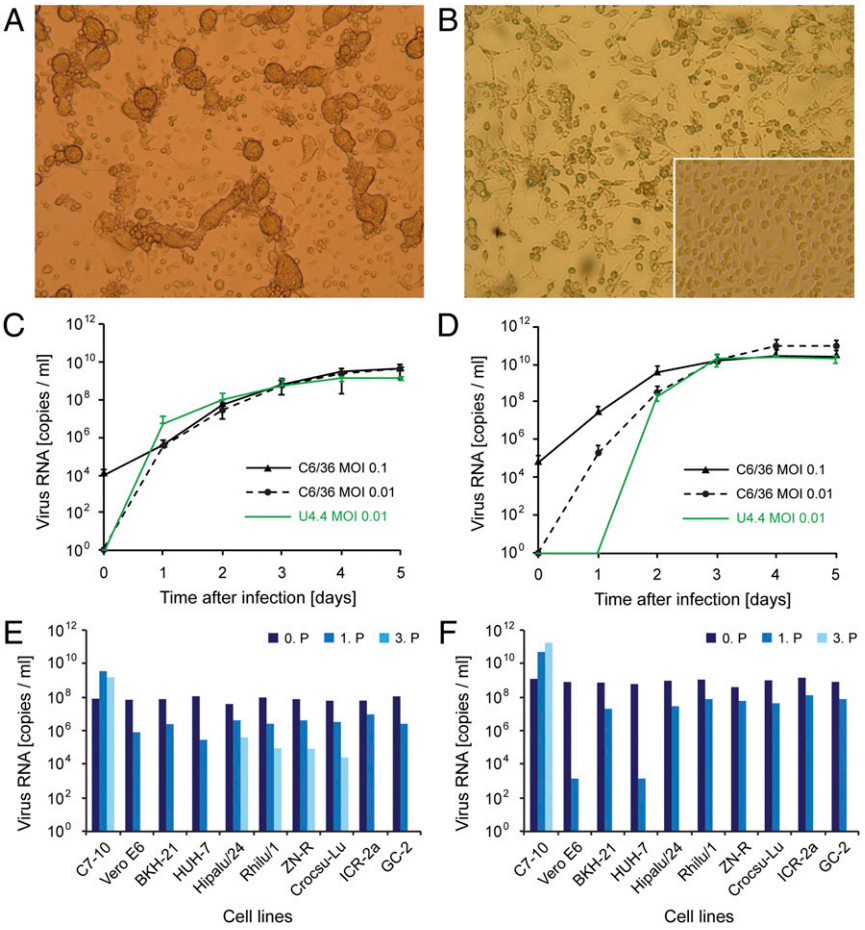

Fig. S1. Growth and cytopathic effects of JONV and FERV. (*A* and *B*) Cytophatic effects of JONV-infected (*A*) and FERV-infected (*B*) C6/36 insect cells 5 dpi. Mock-infected cells are shown in a smaller picture in *B*. (*C* and *D*) Growth analysis of JONV (*C*) and FERV (*D*) on C6/36 cells infected at MOIs of 0.1 and 0.01. U4.4 cells were infected at an MOI of 0.01. The genome copy numbers per milliliter cell culture supernatants were measured for 5 d by real-time RT-PCR. (*E* and *F*) Growth of JONV (*E*) and FERV (*F*) on insect (C7/10) and different vertebrate cells. Cells were infected at an MOI of 1, and three blind passaged were performed after 7 dpi. Genome copy numbers in cell culture supernatants were measured via real-time RT-PCR after passages 0, 1, and 3.

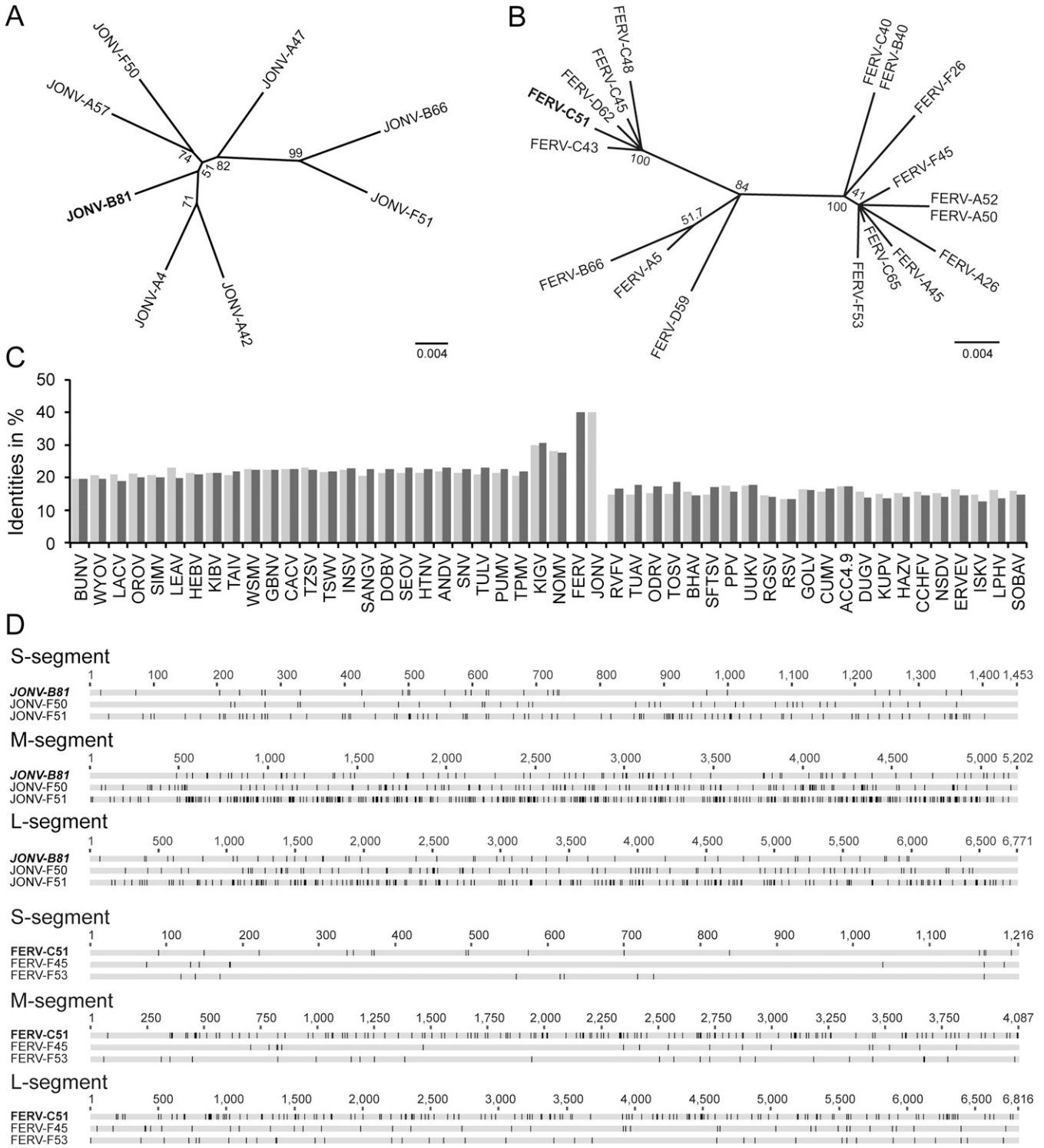

Fig. S2. Phylogenetic relationship and single-nucleotide polymorphisms of JONV and FERV isolates, as well as genetic distances of JONV and FERV to other bunyaviruses. (*A* and *B*) Maximum likelihood analyses of JONV (*A*) and FERV (*B*) isolates performed on a MAFFT-E nucleotide alignment comprising the conserved palm domains of the RdRp. (*C*) Genetic distances of JONV and FERV to representative bunyaviruses based on a structural alignment of RdRp proteins. (*D*) Full-genome analysis of single-nucleotide polymorphisms of JONV and FERV isolates. Nucleotide mutations are illustrated as black bars. Nucleotide substitutions (nonsynonymous and synonymous) were determined for the N and NSs ORFs, using the Datamonkey webserver (1). Mean dN-dS ratio estimation was performed using the SLAC codon-based maximum likelihood method and HKY85 substitution model. NSs and N ORFs had similar values (JONV NSs = −0,919; n = −0,919; FERV NSs = −1; n = −1; FERV NSs = −1).

1. Delport W, Poon AF, Frost SD, Kosakovsky Pond SL (2010) Datamonkey 2010: A suite of phylogenetic analysis tools for evolutionary biology. *Bioinformatics* 26(19):2455–2457.

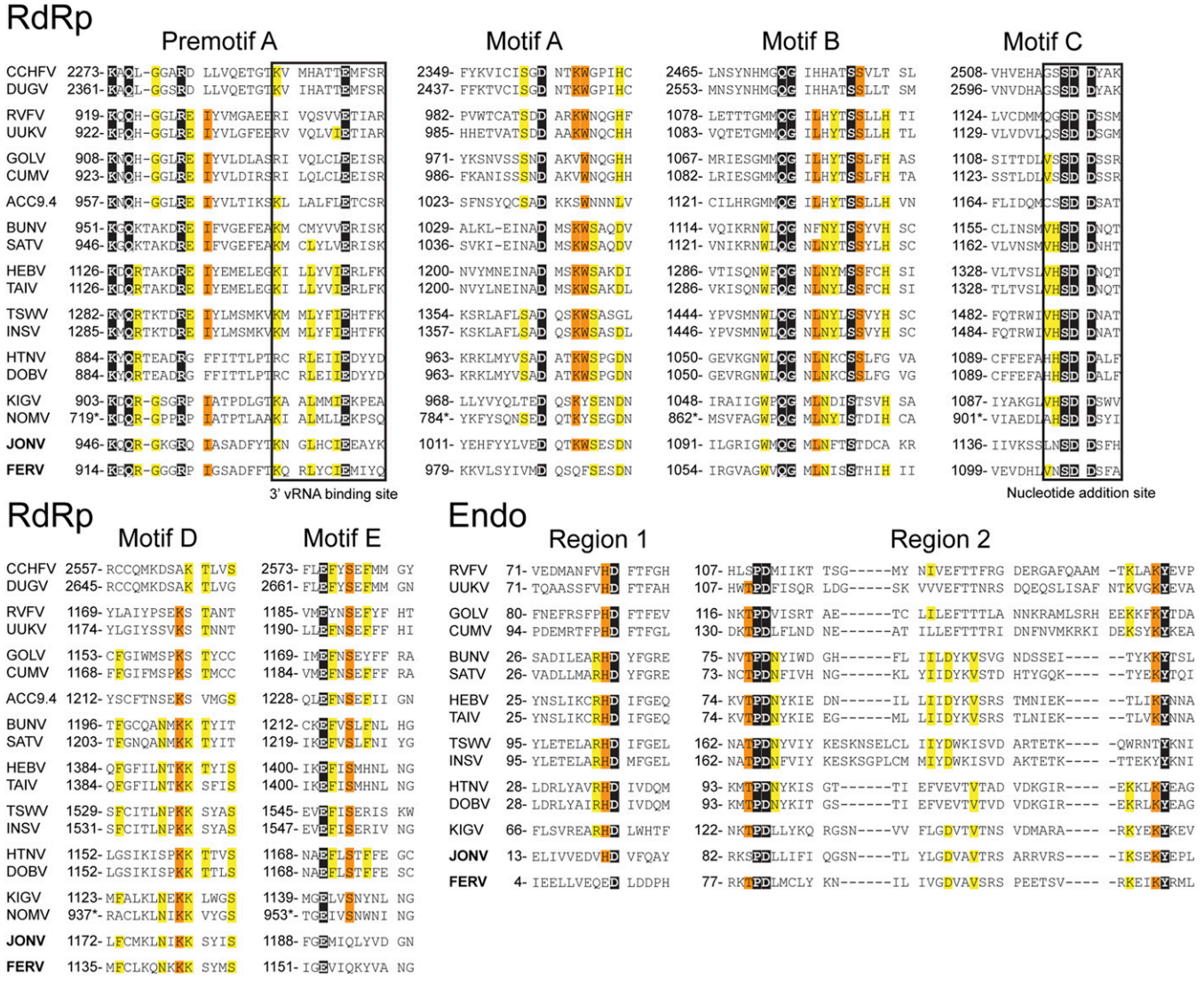

Fig. S3. Multiple-sequence alignments of conserved motifs of the RNA-dependent RNA polymerase (RdRp) and the endonuclease (Endo). Alignments of JONV and FERV with representative bunyaviruses were performed using Expresso in T-Coffee (1). Amino acids with 100% similarity are highlighted in black, those with 75% similarity in orange, and those with 50% similarity in light yellow. Conserved functional domains are annotated. Numbers represent genome positions.

1. Notredame C, Higgins DG, Heringa J (2000) T-Coffee: A novel method for fast and accurate multiple sequence alignment. *J Mol Biol* 302(1):205–217.

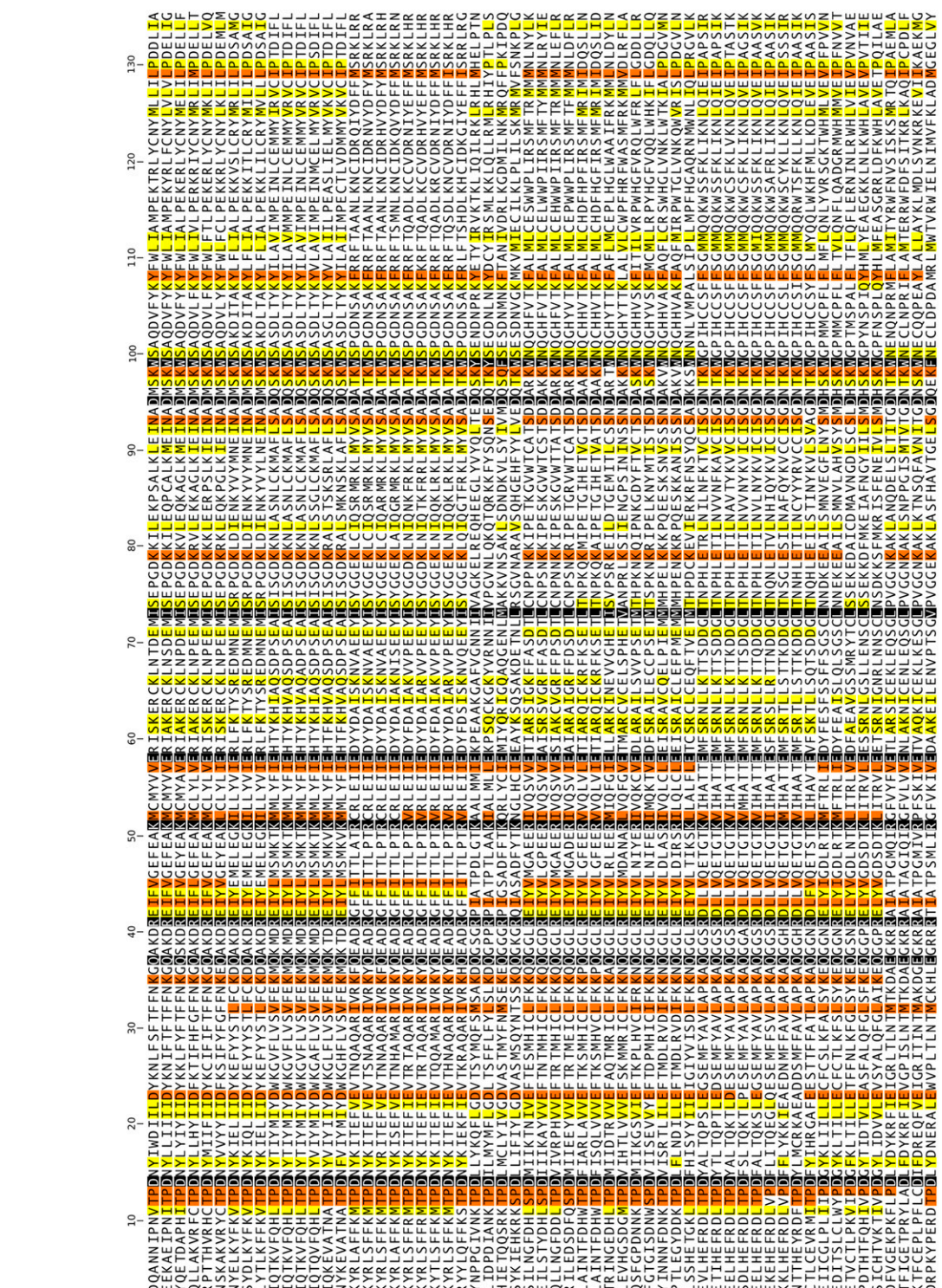

Fig. S4. (Continued)

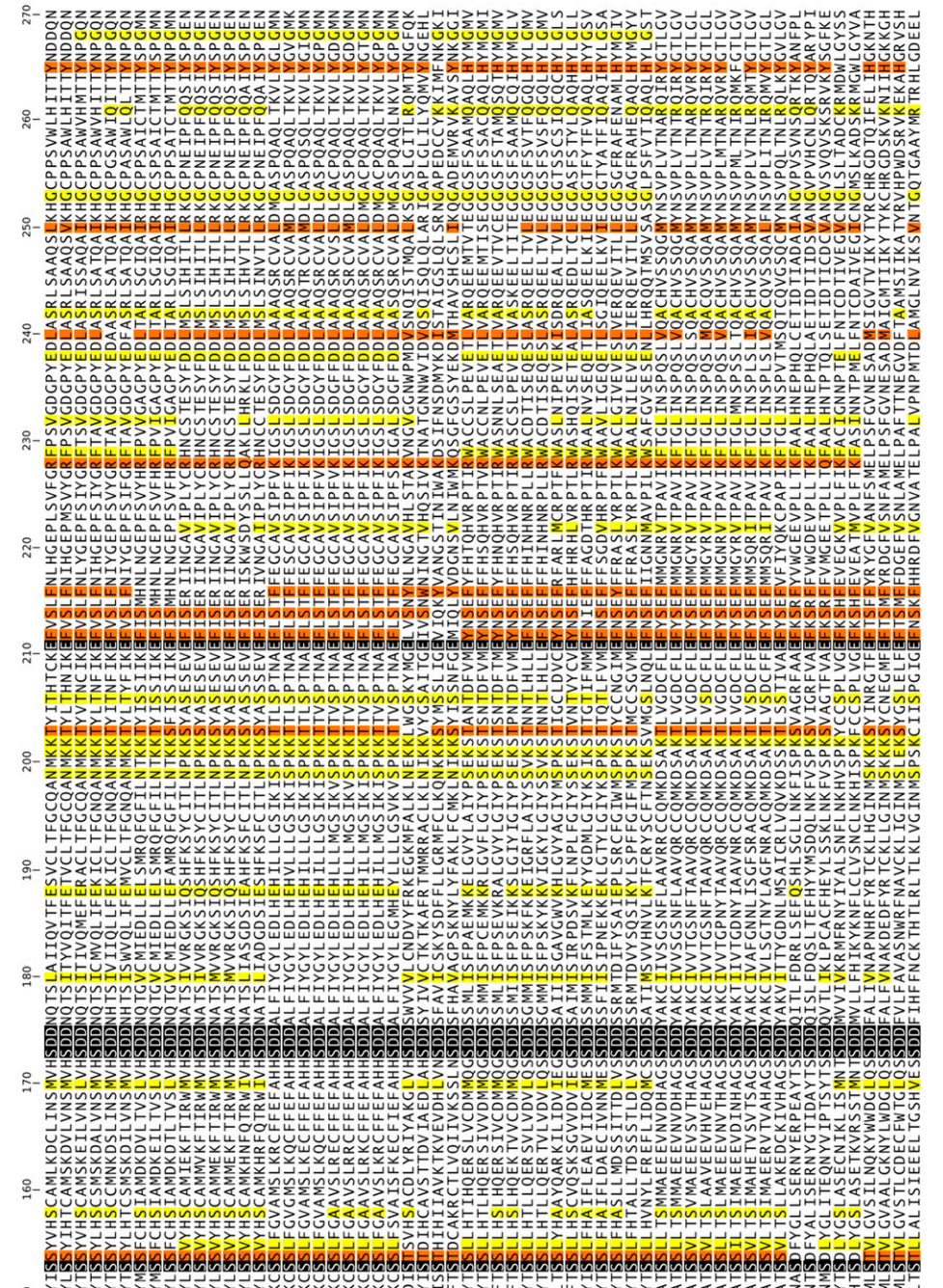

Fig. S4. Alignment of polymerase protein sequences of bunyaviruses, arenaviruses, and orthomyxoviruses. Bunyavirus and arenavirus L segment sequences were aligned with concatenated orthomyxo PA and pb1 segment sequences using the Expresso structural alignment algorithm on the TCoffee webserver (1). The alignment was reduced manually to conserved columns. Black, 100% similar; orange, 80–100% similar; yellow, 60–80% similar; white, less than 60% similar.

1. Notredame C, Higgins DG, Heringa J (2000) T-Coffee: A novel method for fast and accurate multiple sequence alignment. *J Mol Biol* 302(1):205–217.

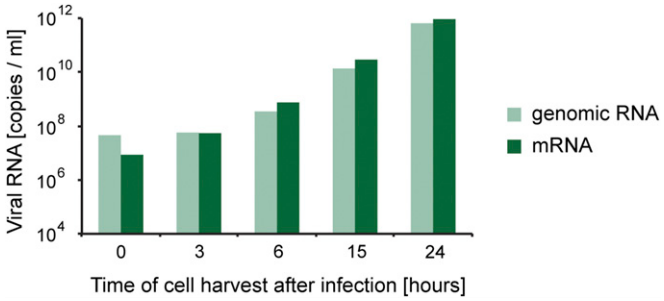

Fig. S5. RNA species during JONV replication in insect cells. Total RNA was extracted at 0, 3, 6, 15, and 24 hpi from C6/36 cells infected with JONV at a MOI of 1. Strain-specific cDNA was synthesized, and amounts of positive and negative sense viral RNA were quantified by real-time RT-PCR.

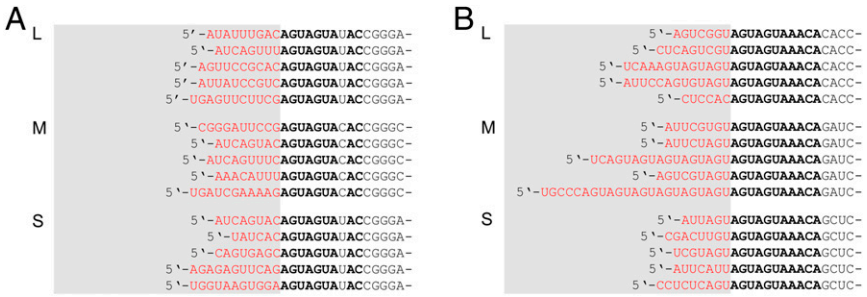

Fig. S6. Nontemplated sequences of JONV and FERV mRNAs. 5′ genome termini of L, M, and S segment mRNAs of JONV (*A*) and FERV (*B*) are shown. Total RNA was extracted at 1 dpi from FERV- and JONV-infected C6/36 cells, respectively. Genome termini were amplified using 5′ RACE-PCR, PCR products were cloned, and five randomly chosen clones were analyzed. Putative transcription primers obtained from host cell mRNAs (nontemplated sequences) are marked in red. Conserved genome termini of FERV and JONV are shown in bold.

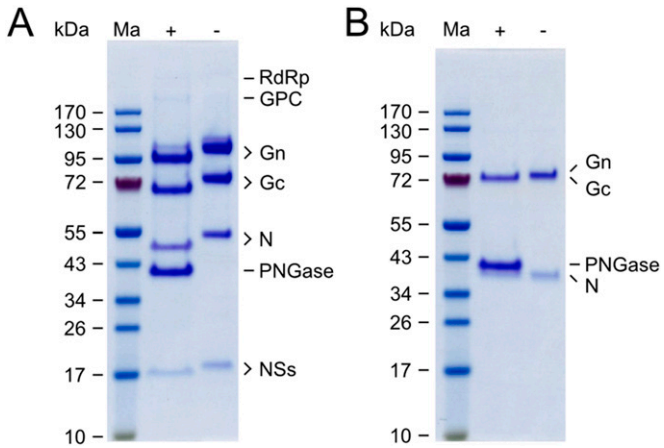

Fig. S7. *N*-linked glycosylation analysis of JONV and FERV proteins. Analysis of JONV (*A*) and FERV (*B*) proteins either treated with (+) Peptide-*N*-glycosidase F or not treated (–). Proteins were separated by SDS/PAGE and stained with Coomassie blue.

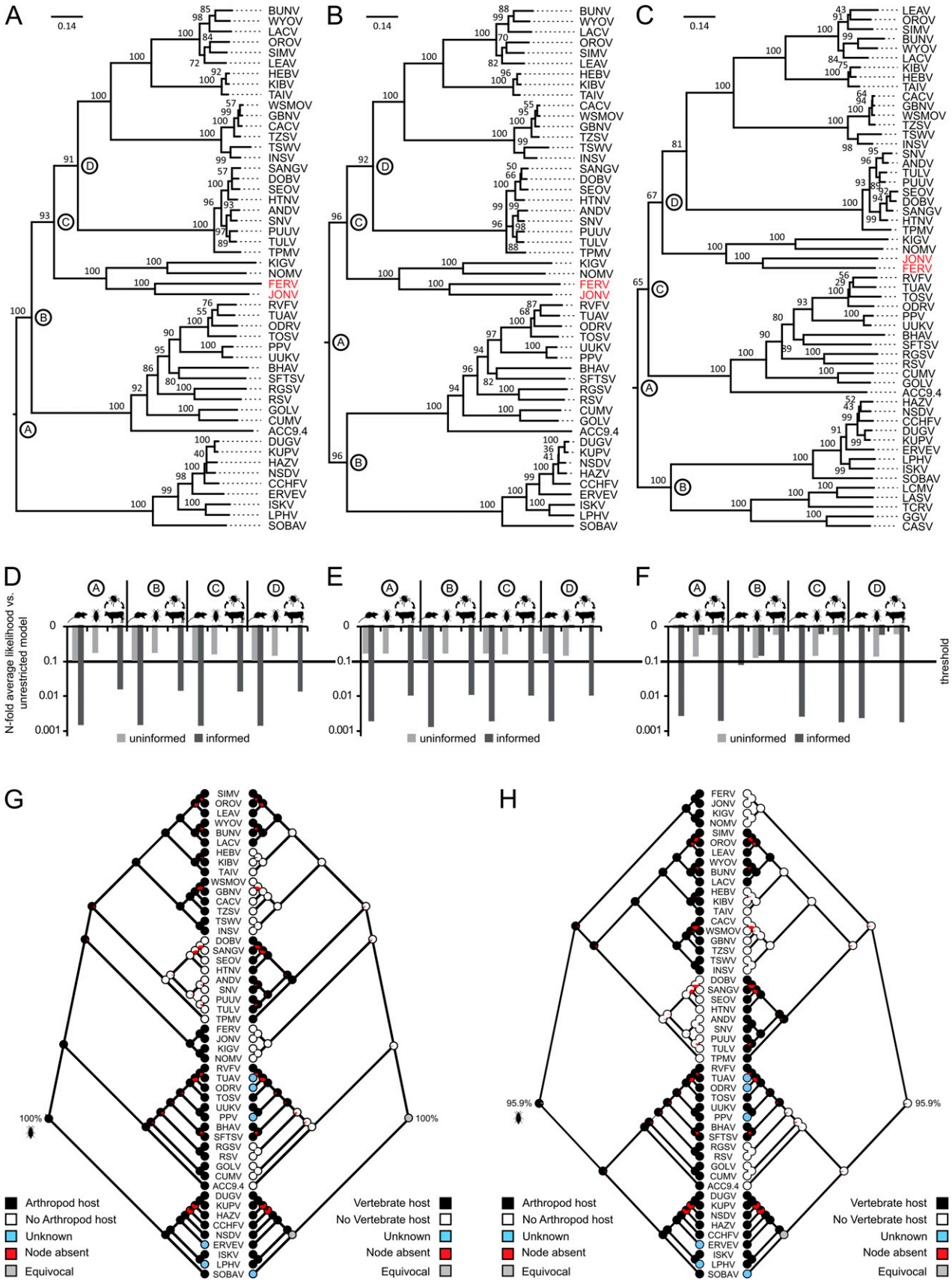

Fig. S8. Phylogenetic reconstructions based on alternative bunyavirus tree topologies. (*A*–*C*) Maximum likelihood phylogeny of conserved L protein domains of bunyaviruses with nairoviruses as a defined basal taxon (*A*) or midpoint rooted with phleboviruses and nairoviruses as sisterclades (*B*), or midpoint rooted

Legend continued on following page

with arenaviruses and nairoviruses as basal sister taxa (*C*). Bootstrap values of 1,000 replicates are indicated at tree nodes. (*D–F*) Probalistic host reconstructions for the tree topologies shown in *A–C*. Hypothesized (fossilized) ancestral host assumptions at deep tree nodes *A–D* are symbolized by vertebrate and arthropod silhouettes. Bars represent the resulting loss of likelihood of trait change models conferred by fossilization (averaged results over 1,000 bootstrap tree replicates). The significance threshold was 10-fold loss of likelihood. (*G* and *H*) Parsimony-based ancestral reconstructions of arthropod and vertebrate host associations for tree topology shown in *A* and *B*. For parsimony-based ancestral reconstructions based on tree topology shown in *C*, refer to Fig. 5 *A* and *B*. LCMV is the type species of the family *Arenaviridae*. Arenaviruses chronically infect rodents and snakes and are transmitted by contact with excretions. Abbreviations (and GenBank accession numbers) are as follows: ACC9.4, uncultured virus isolate acc_9.4 (KF298274); ANDV, Andes virus (NC_003468); BHAV, Bhanja virus (JX961619); BUNV, Bunyamwera virus (NC_001925); CACV, capsicum chlorosis virus (NC_008302); CASV, CAS virus (NC_018484); CCHFV, Crimean-Congo hemorrhagic fever virus (NC_005301); CUMV, Cumuto virus (KF543244); DOBV, Dobrava virus (NC_005235); DUGV, Dugbe virus (NC_004159); ERVEV, Erve virus (JF911697); FLUAV, influenza A virus (NC_002021); FLUBV, influenza B virus (NC_002204); FLUCV, influenza C virus (NC_006308); GBNV, groundnut bud necrosis virus (NC_003614); GGV, Golden Gate virus (NC_018482); GOLV, Gouléako virus (HQ541738); HAZV, Hazara virus (DQ076419); HEBV, Herbert virus (JQ659256); HTNV, Hantaan virus (NC_005222); INSV, impatiens necrotic spot virus (NC_003625); ISKV, Issyk-Kul virus (KF892055); KIBV, Kibale virus (KF590577); KIGV, Kigluaik phantom virus (KJ434182); KUPV, Kupe virus (EU816899); LACV, La Crosse virus (NC_004108); LASV, Lassa virus (NC_004297); LCMV, Lymphocytic choriomeningitis virus (NC_004291); LEAV, Leanyer virus (HM627178); LPHV, Leopards Hill virus (AB842091); NOMV, Nome phantom virus (KJ434185); NSDV, Nairobi sheep disease virus (EU697949); ODRV, Odrenisrou virus (HM566174); OROV, Oropouche virus (NC_005776); PPV, precarious point virus (HM566181); PUUV, Puumala virus (NC_005225); RGSV, rice grassy stunt virus (NC_002323); RSV, rice stripe virus (NC_003755); RVFV, Rift Valley fever virus (NC_014397); SANGV, Sangassou virus (JQ082302); SEOV, Seoul virus (NC_005238); SFTSV, severe fever with thrombocytopenia syndrome virus (NC_018136); SIMV, Simbu virus (NC_018476); SNV, Sin Nombre virus (NC_005217); SOBAV, South Bay virus (KM048320); TAIV, Taï virus (KF590574); TCRV, Tacaribe virus (NC_004292); THOV, Thogoto virus (NC_006495); TPMV, Thottapalayam virus (NC_010707); TOSV, Toscana virus (NC_006319); TSWV, tomato spotted wilt virus (NC_002052); TULV, Tula virus (NC_005226); TUAV, Turuna virus (HM119431); TZSV, tomato zonate spot virus (NC_010491); UUKV, Uukuniemi virus (NC_005214); WSMOV, watermelon silver mottle virus (NC_003832); WYOV, Wyeomyia virus (JN572080).

Table S1. Trait matrix used for ancestral reconstructions

	Uninformed		Informed	
Virus	Arthropod	Vertebrate	Arthropod	Vertebrate
BUNV	1	1	1	1
WYOV	1	1	1	1
LACV	1	1	1	1
OROV	1	1	1	1
SIMV	1	1	1	1
LEAV	1	1	1	1
HEBV	1	n.k.	1	0
KIBV	1	n.k.	1	0
TAIV	1	n.k.	1	0
WSMOV	1	0	1	0
GBNV	1	0	1	0
CACV	1	0	1	0
TZSV	1	0	1	0
TSWV	1	0	1	0
INSV	1	0	1	0
SANGV	0	1	0	1
DOBV	0	1	0	1
SEOV	0	1	0	1
HTNV	0	1	0	1
ANDV	0	1	0	1
SNV	0	1	0	1
PUUV	0	1	0	1
TULV	0	1	0	1
TPMV	0	1	0	1
KIGV	1	n.k.	1	0
NOMV	1	n.k.	1	0
FERV	1	n.k.	1	0
JONV	1	n.k.	1	0
RVFV	1	1	1	1
TUAV	1	n.k.	1	n.k.
ODRV	1	n.k.	1	n.k.
TOSV	1	1	1	1
PPV	1	n.k.	1	n.k.
UUKV	1	1	1	1
BHAV	1	1	1	1
SFTSV	1	1	1	1
RGSV	1	0	1	0
RSV	1	0	1	0
GOLV	1	n.k.	1	0
CUMV	1	n.k.	1	0
ACC9.4	1	n.k.	1	0
DUGV	1	1	1	1
KUPV	1	1	1	1
HAZV	1	1	1	1
NSDV	1	1	1	1
CCHFV	1	1	1	1
ERVEV	n.k.	1	n.k.	1
ISKV	1	1	1	1
LPHV	n.k.	1	n.k.	1
SOBAV	1	n.k.	1	n.k.
LCMV	0	1	0	1
LASV	0	1	0	1
TCRV	1	1	1	1
CASV	n.k.	1	n.k.	1
GGV	n.k.	1	n.k.	1

ACC9.4, uncultured virus isolate acc_9.4 (KF298274); ANDV, Andes virus (NC_003468); BHAV, Bhanja virus (JX961619); BUNV, Bunyamwera virus (NC_001925); CACV, capsicum chlorosis virus (NC_008302); CCHFV, Crimean-Congo hemorrhagic fever virus (NC_005301); CUMV, Cumuto virus (KF543244); DOBV, Dobrava virus (NC_005235); DUGV, Dugbe virus (NC_004159); ERVEV, Erve virus (JF911697); GBNV, groundnut bud necrosis virus (NC_003614); GOLV, Gouléako virus (HQ541738); HAZV, Hazara virus (DQ076419); HEBV, Herbert virus (JQ659256); HTNV, Hantaan virus (NC_005222); INSV, Impatiens necrotic

spot virus (NC_003625); ISKV, Issyk-Kul virus (KF892055); KIBV, Kibale virus (KF590577); KIGV, Kigluaik phantom virus (KJ434182); KUPV, Kupe virus (EU816899); LACV, La Crosse virus (NC_004108); LEAV, Leanyer virus (HM627178); LPHV, Leopards Hill virus (AB842091); n.k. = not known; NOMV, Nome phantom virus (KJ434185); NSDV, Nairobi sheep disease virus (EU697949); ODRV, Odrenisrou virus (HM566174); OROV, Oropouche virus (NC_005776); PPV, precarious point virus (HM566181); PUUV, Puumala virus (NC_005225); RGSV, rice grassy stunt virus (NC_002323); RSV, rice stripe virus (NC_003755); RVFV, Rift Valley fever virus (NC_014397); SANGV, Sangassou virus (JQ082302); SEOV, Seoul virus (NC_005238); SFTSV, severe fever with thrombocytopenia syndrome virus (NC_018136); SIMV, Simbu virus (NC_018476); SNV, Sin Nombre virus (NC_005217); SOBAV, South Bay virus (KM048320); TAIV, Taï virus (KF590574); TPMV, Thottapalayam virus (NC_010707); TOSV, Toscana virus (NC_006319); TSWV, tomato spotted wilt virus (NC_002052); TULV, Tula virus (NC_005226); TUAV, Turuna virus (HM119431); TZSV, tomato zonate spot virus (NC_010491); UUKV, Uukuniemi virus (NC_005214); WSMOV, watermelon silver mottle virus (NC_003832); WYOV, Wyeomyia virus (JN572080).